POLITECNICO DI TORINO
Repository ISTITUZIONALE

Impact of controlled vacuum induced surface freezing on the freeze drying of human plasma

Original
Impact of controlled vacuum induced surface freezing on the freeze drying of human plasma / Arsiccio, A.; Matejtschuk, P.; Ezeajughi, E.; Riches-Duit, A.; Bullen, A.; Malik, K.; Raut, S.; Pisano, R.. - In: INTERNATIONAL JOURNAL OF PHARMACEUTICS. - ISSN 0378-5173. - STAMPA. - 582:(2020), p. 119290. [10.1016/j.ijpharm.2020.119290]

Availability:
This version is available at: 11583/2862732 since: 2021-01-18T16:20:13Z

Publisher:
Elsevier B.V.

Published
DOI:10.1016/j.ijpharm.2020.119290

Terms of use:

This article is made available under terms and conditions as specified in the corresponding bibliographic description in the repository

Publisher copyright
Elsevier postprint/Author's Accepted Manuscript

© 2020. This manuscript version is made available under the CC-BY-NC-ND 4.0 license
http://creativecommons.org/licenses/by-nc-nd/4.0/.The final authenticated version is available online at:
http://dx.doi.org/10.1016/j.ijpharm.2020.119290

(Article begins on next page)

02 May 2024

Authors' post-prints

Arsiccio, A., Matejtschuk, P., Ezeajughi, E., Riches-Duit, A., Bullen, A., Malik, K., Raut, S., Pisano, R. (2020). Impact of Controlled Vacuum Induced Surface Freezing on the Freeze Drying of Human Plasma. International Journal of Pharmaceutics **582**(*30*), article no. 119290.

* Corresponding author: roberto.pisano@polito.it

Impact of Controlled Vacuum Induced Surface Freezing on the Freeze Drying of Human Plasma

Andrea Arsiccio[1], Paul Matejtschuk[2], Ernest Ezeajughi[2], Andrew Riches-Duit[4], Anwen Bullen[3,5], Kiran Malik[2], Sanj Raut[4] & Roberto Pisano[1].

1. Department of Applied Science and Technology, Politecnico di Torino, 24 corso Duca degli Abruzzi, Torino, 10129 Italy.
2. Standardisation Science & 3. Imaging Section, Analytical & Biological Sciences Division & 4. Biotherapeutics Division, National Institute for Biological Standards & Control (NIBSC), Blanche Lane, South Mimms, Potters Bar, Hertfordshire, United Kingdom , EN6 3QG.
5. UCL Ear Institute, Gray's Inn Road, London, UK, WC1X 8EE

Email address of corresponding author : Paul.Matejtschuk@nibsc.org

ABSTRACT

During the freezing step of a typical freeze drying process, the temperature at which nucleation is induced is generally stochastically distributed, resulting in undesired within-batch heterogeneity. Controlled nucleation techniques have been developed to address this problem; these make it possible to trigger the formation of ice crystals at the same time and temperature in all the batch. Here, the controlled nucleation technique known as vacuum induced surface freezing is compared to spontaneous freezing for the freeze drying of human plasma, a highly concentrated system commonly stored in a dried state. The potency of Factor VIII (FVIII), a sensitive, labile protein present in plasma, and the reconstitution time of the dried cakes are evaluated immediately after freeze drying, and after 1, 3, 6 or 9 months storage at different degradation temperatures. We show that the application of controlled nucleation significantly reduces the reconstitution time and in addition helps to improve FVIII stability.

KEYWORDS: freeze drying, controlled nucleation, plasma, biological activity

ABBREVIATIONS: VISF: Vacuum Induced Surface Freezing

1. INTRODUCTION

The freeze-drying process is widely used for preserving labile products in the pharmaceutical industry, by removal of water at low temperature to increase shelf life, without significantly affecting the therapeutic properties of the active ingredients (Fissore, 2019; Franks and Auffret, 2007; Rey and May, 2010; Ward and Matejtschuk, 2019). During freeze drying, the product is first frozen, and water is subsequently removed by sublimation during primary drying and desorption during secondary drying. The two drying phases are performed at low pressure, the first typically at sub-zero temperature, so as to minimize possible degradation stresses.

In the field of pharmaceutical freeze drying, where often many thousands of vials or ampoules are processed in a single cycle, the problem of potential heterogeneity within each batch is a major concern. Much of this heterogeneity is related to the freezing step, and specifically to the uncontrolled, random distribution of nucleation temperatures within the batch. The nucleation temperature determines the morphology of the final product, with a high nucleation temperature resulting in larger ice crystals (Searles et al., 2001). In turn, the ice crystal size corresponds to the pore size of the dried product, provided that no

collapse occurs, and has therefore an impact on process efficiency (Capozzi and Pisano, 2018; Hottot et al., 2007; Kasper and Friess, 2011; Pikal et al., 2002). For instance, a large pore size speeds up the removal of water by sublimation, reducing the primary drying time, but results in a slow desorption rate during secondary drying (Oddone et al., 2016; Oddone et al., 2017).

A small ice crystal size also results in the formation of a large ice-water interface, where amphiphilic molecules, such as proteins, could get adsorbed and unfold because of their interaction with the surface (Strambini and Gabellieri, 1996). This surface-induced stress adds up to the risk of cold denaturation (Franks, 1995; Privalov, 1990) that may occur because of the low temperature used during freezing, and it has been shown that for many proteins it actually is the main source of protein instability during the freezing process (Bhatnagar et al., 2008; Chang et al., 1996). Finally, the pore size of a dried product also affects the reconstitution time, which is not a negligible factor to be considered, especially for highly concentrated products. While low-concentration formulations generally reconstitute in less than 1 min (Lewis et al., 2010), it may take up to 1 h for higher concentrated systems to yield an injectable solution (Shire et al., 2004), which can be a critical issue clinically.

The possibility to control the nucleation temperature during freeze drying would therefore make it possible to modulate the overall process efficiency, and the critical attributes of the final product as well. Moreover, the batch homogeneity, which is a key requirement in the pharmaceutical and reference standard industries, may be improved. It is therefore not surprising that various techniques have been developed over the years to address this problem (Geidobler and Winter, 2013; Kasper, 2011; Pisano, 2019). Recent studies have shown that induced nucleation has no deleterious effects and can even improve the lyophilization of model proteins such as LDH (Fang et al., 2018), monoclonal antibodies (MAbs) (Awotwe-Otoo et al., 2013) and human growth hormone (Oddone et al., 2020). In this study we will look at the impact of induced nucleation on the reconstitution time of human plasma after freeze drying and the recovery of Factor VIII activity in that plasma. Coagulation Factor VIII (FVIII:C) is the most labile haemostatic protein, whose activity is routinely used to study/assess protein stability in plasma (Allain JP et al., 1983; Carlebjörk G et al., 1986; Takahashi H et al., 1986; Swärd-Nilsson AM et al., 2006).

One commercially available solution the ice-fog technique (Brower et al., 2015; Geidobler et al., 2012; Patel et al, 2009; Rambhatla et al., 2004), uses small ice particles, generated by the release of cold nitrogen within the freezing chamber and that penetrate into the vials, to trigger ice nucleation. This ice fog could also be generated within an external condenser, or another cold chamber. Vacuum could be established in the freeze-dryer, while maintaining the condenser at atmospheric pressure. When connection is established

between the dryer and the condenser, the ice fog is transported into the drying chamber, inducing nucleation (Ling, 2014; Umbach, 2017). Another approach, based on rapid pressurization/depressurization of the drying chamber, may also be used (Bursac et al., 2009; Gasteyer et al., 2017; Konstantinidis et al., 2011). However, not all freeze dryers can accommodate the overpressuring required to apply this high-pressure-shift or depressurization method.

In this work, the so-called vacuum induced surface freezing (VISF) technique, also known as vacuum induced nucleation (VIN), will be used. In VISF, a reduction in chamber pressure is used to trigger ice formation in products that have been previously equilibrated at the desired nucleation temperature (T_n). The nucleated samples are then held for a given amount of time (generally about 1 h) at the same or another temperature (T_m) to promote the formation of large ice crystals. This results in a larger pore size, faster primary drying rate, and reduced ice-water surface area compared to conventional freezing. This method was first proposed by Kramer et al. (2002), and later used by other groups (Arsiccio et al., 2018; Liu et al., 2005; Oddone et al., 2014; Oddone et al., 2016; Oddone et al., 2017). Representative profiles of fluid temperature and chamber pressure during application of this technique are shown in Figure 1.

Here, the method by Oddone et al. (2014; 2016; 2017), will be applied to human plasma, a highly concentrated system that is commonly freeze dried. In the context of freeze-drying, the term high-concentration protein formulation is generally applied to preparations ranging from 50 to about 150 mg/ml of protein (Garidel and Presser, 2019). This type of formulations typically shows increased viscosities, high opalescence, phase separation or particle formation phenomena that are uncommon in low-concentration preparations. Human plasma can perfectly fit into this definition, as it contains a huge amount of proteins. Among them, FVIII is an essential clotting factor whose impaired function results in haemophilia A, a rare, sex-linked bleeding disorder. FVIII is a labile plasma protein, which is particularly sensitive to denaturation stresses. The effect of controlled nucleation on the stability of FVIII will be investigated, and a comparison will be made with spontaneous freezing. This analysis will be performed both immediately after freeze drying, and after 1, 3, 6 or 9 months accelerated degradation stability study at different temperatures (Kirkwood, 1977; Kirkwood, 1984; Kirkwood and Tydeman, 1984). The reconstitution time of the dried cakes obtained after the two freezing protocols will also be assessed.

2. MATERIALS AND METHODS

2.1 Material for filling

Screened human plasma (Blood Group: A+, National Blood & Transplant, Colindale, UK) was thawed and Hepes (free acid H3375, Sigma Merck, Poole, UK) was added to a final concentration of 40 mM and the bulk held over ice with gentle stirring. Batches of one ml aliquots were dispensed using a Hamilton autodilutor (Hamilton M510B, supplied by Microlab Technologies Ltd, Westcliff -on Sea, UK) into 5 ml ampoules (glass type I, Schott supplied by Adelphi Tubes, Haywards Heath, UK) and fitted with 13mm diameter halobutyl rubber lyo-closures (West Pharma, supplied by Adelphi) – partially inserted to allow sublimation to occur. A batch of 100 ampoules was prepared on each of two occasions and the coefficient of variation (CV) of fill assessed by measuring empty, filled and dried weights on three ampoules across the batch. The ampoules were then loaded directly onto a freeze dryer (LyoBeta 15, Telstar Azbil SpA, Terrassa, Spain) and the freeze drying cycle begun.

2.2 Freeze drying cycle

Two consecutive cycles were performed, one with spontaneous nucleation and one with VISF controlled nucleation. During the VISF cycle, the product was first equilibrated at -5 °C for about 1 h. The pressure was then reduced to a low value (about 1 mbar), promoting a strong evaporation from the ampoules, and therefore a decrease in temperature that triggered nucleation. As soon as nucleation was induced in all ampoules, pressure was quickly released to the atmospheric value to avoid boiling of the solution. The product was then equilibrated at -10 °C for about 45 min before the final ramp to -50 °C. The combination T_n=-5°C, T_m=-10°C was selected based on previous observations (Oddone et al., 2016), where different values for both equilibration temperatures were tested. T_n=-5°C should guarantee the formation of large ice crystals. Lower temperature values (e.g, -10°C) were found to result in a smaller crystal size, while, for instance, T_n=+5°C increased the within-ampoule heterogeneity. Different values of T_m were also compared [Oddone et al., 2016]. It was observed than when T_m was too high, for instance equal to -5°C, the solution could not freeze completely during the holding stage, and thus froze as soon as the temperature of the heat transfer fluid was decreased to -45/-50°C. This resulted in smaller ice crystals, and therefore larger ice-water surface area, within the product. By contrast, T_m=-10°C improved the situation, promoting the formation of large ice crystals during the holding step and avoiding melting back phenomena. For spontaneous freezing, a continuous 0.5 °C/min ramp to -50 °C was performed.

For both the spontaneous and the VISF cycle, the product was held at -50 °C for 3 h to complete freezing. The product was then held at -50 °C for 1 h at 0.2 mbar , and for 1 h at 0.1 mbar. The temperature was subsequently raised to -12 °C in 1 h and held at 0.1 mbar for 30 h. Secondary drying was eventually performed at 25 °C for 20 h. A 10 h ramp between primary and secondary drying was used. After the cycle the dryer was back-filled with dry nitrogen (from boil off of pure liquid nitrogen) and the closures stoppered down before ampoules were removed from the dryer. Ampoules were then flame-sealed using a manual ampoule sealer (Ampulmatic, Adelphi Tubes).

A scheme of the protocols used for freeze drying is shown in Table 1.

Table 1. Scheme of the experimental protocols used in this work for the freeze drying of human plasma. SPON: spontaneous nucleation, VISF: vacuum induced surface freezing.

	VISF			SPON		
Step	T, °C	P, mbar	t, h	T, °C	P, mbar	t, h
Freezing						
holding	-5	-	1	-	-	-
nucleation	-5	~1	-	-	-	-
holding	-10	-	0.75	-	-	-
ramp	-50	-	1	-50	-	1.5
holding	-50		3	-50	-	3

	SPON/VISF		
	T, °C	P, mbar	t, h
Primary Drying			
holding	-50	0.2	1
holding	-50	0.1	1
ramp	-12	0.1	1
holding	-12	0.1	30
Secondary Drying			
ramp	25	0.1	10
holding	25	0.1	20

In each batch, the temperature profile inside one ampoule was monitored by means of T-type copper/constantan miniature thermocouples placed at the bottom centre of the vial, and touching the bottom. During drying, both a capacitance (MKS Baratron) and a thermal conductivity (Pirani) manometer were used to monitor the pressure inside the drying chamber. The capacitance manometer always outputs the exact value of pressure within the chamber, while the Pirani gauge readings are shifted to higher values during primary drying. When the Pirani sensor readings begin to decay, the onset time is reached, indicating that a significant number of ampoules have completed the sublimation process (Patel et al., 2010). When the readings of the Pirani and Baratron manometers eventually converge, the offset time is reached, indicating

that sublimation has ended in all the batch (see Figure 2). The offset time can be considered as the end of the primary drying phase, while the difference between offset time and onset time (in the following referred to as onset-offset time) is a measure of within-batch heterogeneity. The larger this difference the greater the difference in sublimation behavior of ampoules within the batch.

2.3 FVIII assay, reconstitution times and stability study

FVIII chromogenic assays, for potency determination of FVIII in ampoules prepared by the two different freezing protocols, were carried out on the ACLTOP 550 analyzer (Werfen Ltd., Birchwood, UK) using the Coatest SP4 FVIII chromogenic kit (Chromogenix, Werfen Ltd., Birchwood, UK), according to European Pharmacopoeia guidelines (Ph. Eur. monograph Human coagulation factor VIII - 0275). Briefly, optimal amounts of calcium and phospholipids, and excess amounts of factors IXa (FIXa) and X (FX) were added to the reconstituted test sample containing the FVIII analyte, and under these conditions, factor X is converted to FXa by FIXa, where the rate of FX activation is dependent on the amount of FVIII present in the test sample. The FXa generated hydrolyses the chromogenic substrate and the amount of colour produced is read photometrically at 405 nm. The intensity of colour is therefore proportional to the amount of FVIII in the test sample.

For the stability studies, freeze dried ampoules of human plasma containing FVIII were put down for storage at degradation temperatures of +45°C, +37°C, +20°C, +4°C and -20°C. Assessment of the stability of the FVIII was carried out through accelerated degradation studies which allow the prediction of degradation rates of samples stored at low temperatures (e.g. -20°C) based on the observed loss in potency of samples stored at elevated temperatures (e.g. +4, +20, +37, +45 °C) (Kirkwood, 1977). This is an indirect method used routinely to determine rate of loss based on the Arrhenius equation, where a first order reaction rate is assumed (Kirkwood, 1984; Kirkwood and Tydeman, 1984).

Test ampoules were retrieved from different storage temperatures, at different time points and each ampoule was reconstituted as described in the current European Pharmacopoeia guideline, (Ph. Eur. general chapter section - assay of human coagulation factor VIII, monograph 2.7.4). Briefly, to each test ampoule, 1 ml sterile water was added followed by gentle swirling and then allowed to stand at ambient temperature until dissolved.

The time for full reconstitution was obtained for the two different freezing protocols. The reconstituted samples were then assayed on the ACLTOP 550 analyser, where each sample was diluted (1/50, 1/100 & 1/200) in kit buffer in duplicates prior to the chromogenic assay run. Assays were carried out relative to the

WHO 6th International Standard (WHO 6th IS) FVIII/VWF Plasma (07/316) for potency estimation or relative to pre-freeze-drying liquid sample for assessment of % loss in potency or relative to the respective -20°C freeze-dried samples to assess stability. Results were analysed using CombiStats software, version 5.0 (1999-2013 EDQM/Council of Europe).

2.4 Scanning electron microscopy analysis

The pore dimensions of the products obtained after freeze-drying was analysed using a Scanning Electron Microscope (SEM). Three samples from both the spontaneous and the VISF cycle were examined. Each sample was cut along the vertical axis of the cake, and a central section was mounted onto aluminium stubs with conductive silver paint (Agar Scientific, Stanstead, UK). Samples were sputter coated with 4nm gold and imaged immediately after mounting. Imaging was carried out by a JSM 7401F SEM (Jeol Ltd, Welwyn Garden City, UK) operating at 5kV. Images were obtained by secondary electron detection. SEM images were recorded at the top, centre and bottom of each cake.

For analysis, approximately 50 pores were selected in each image (at x50 magnification), and each of them was approximated to an ellipse. The diameter of the circle having the same area to perimeter ratio of the approximating ellipse was then assumed as pore dimension, and the numerical average of the obtained distribution was assumed as the average pore size, D_p, of the product.

2.5 BET determination of specific surface area

Nitrogen (N_2) adsorption method was used in a physisorption analyser (ASAP 2020 Plus, Micromeritics, Norcross, GA, USA) to determine the specific surface area (SSA) of freeze dried samples. The samples were degassed for 5 h at 293 K under vacuum. N_2 adsorption isotherms were acquired at 77 K in a P/P_0 (relative pressure) range of 0.005-0.99. For the BET analysis, 12 points in the range P/P_0=0.05-0.30 were then used. In all cases, the sample size was between 250 and 300 mg.

3. RESULTS

3.1 Performance of the Freezing Protocols

The positive effects of VISF on primary drying time, already discussed in the literature (Arsiccio et al., 2018; Oddone et al., 2014; Oddone et al., 2016), were confirmed in this work. As shown in Figure 2a, primary drying lasted about 17.6 h for the spontaneous cycle (difference between offset time and the beginning of the drying process). Moreover, the onset-offset time in this case amounted to about 4.2 h. In contrast, primary

drying was shorter, about 13.1 h, when the VISF technique was applied (Figure 2b). This result is not negligible, as it corresponds to approximately 25.6 % reduction in sublimation time upon application of controlled nucleation. The onset-offset time, which is a measure of variability in sublimation behaviour, also decreased to about 3 h when controlled nucleation was used. This suggests that the application of VISF is beneficial when homogeneity is an issue, and this effect may be even more significant in the case of large industrial-scale batches.

The observed difference in sublimation rate between spontaneous and controlled nucleation may be related to a difference in pore size. The VISF technique made it possible to induce nucleation in all samples at a high temperature (-5 °C), where formation of ice nuclei is still not observed in spontaneously-frozen ampoules. For instance, the thermocouple-containing ampoule during the spontaneous run nucleated at about -15 °C (as shown in the inset of Figure 2a). In turn, a high nucleation temperature translates into the formation of large ice crystals, that subsequently convert into equally large pores when ice is removed during sublimation. The removal of water vapour through these pores occurs with a significantly reduced resistance to mass transfer, boosting the sublimation process.

This hypothesis was confirmed from viewing the SEM images shown in Figure 3, where the VISF technique evidently promoted the formation of larger pores compared to spontaneous nucleation. The images for one sample only are displayed in Figure 3, but the same trend was observed for all the three ampoules analyzed, as detailed in Table 2. The use of microscopy to assess the structure of frozen or freeze dried cakes has been reported several times in the literature (Vollrath et al., 2019; Goshima et al., 2016; Abdul-Fattah et al., 2008), and here the SEM images were also quantitatively analyzed, similarly to what was done in previous works, where frequency domain image analysis (Grassini et al., 2016) or segmentation approaches (Arsiccio et al., 2019) were used for this purpose.

Table 2. Pore dimension D_p (as measured by SEM) and BET specific surface area (as measured by N_2 adsorption) in the dried product, for spontaneous and controlled nucleation (average ± standard deviation). For the BET surface area, two repetitions were made, and both sets of measurements are reported in the last column.

Sample #	Freezing Protocol	D_p, µm			BET surface area, m^2/g
		bottom	centre	top	
1	VISF	118 ± 49	130 ± 68	115 ± 71	0.19 ± 0.01 0.25 ± 0.01
2		120 ± 48	131 ± 58	115 ± 58	
3		104 ± 46	121 ± 47	107 ± 55	
1	Spon.	49 ± 15	65 ± 21	52 ± 13	0.41 ± 0.01 0.40 ± 0.01
2		51 ± 18	65 ± 18	52 ± 13	
3		68 ± 17	68 ± 15	65 ± 15	

Here, the difference in pore dimension was quantified by an image analysis technique, where each pore was approximated to an ellipse, and the diameter of the circle having equal area to perimeter ratio was computed. Averaging over all the samples, the VISF technique resulted in a dried cake with pore size in the order of about 114, 127 and 112 µm at the bottom, centre and top, respectively. The presence of larger pores at the centre of the cake is common during freeze-drying, because the contact with the dryer shelves, and the presence of cryo-concentration effects promote the formation of a less open structure at the cake edges. In contrast, the average values for the spontaneously nucleated samples were lower, about 56, 66 and 56 µm at the bottom, centre and top, indicating that the lower nucleation temperature in these samples approximately halved the pore size compared to the case of the VISF cycle.

The SEM data were confirmed by the BET specific surface area (SSA) values, also listed in Table 2. As expected, a larger pore size obtained when applying controlled nucleation resulted in a smaller SSA, which as will be shown in the following, may have an impact on protein stability.

3.2 FVIII residual activity

In this study, as FVIII is the most labile haemostasis protein in plasma, it was decided that assessment of the functional activity of FVIII in the freeze-dried samples would allow more clearly to discern any differences between the 2 freeze drying techniques. The potency of FVIII was measured post-drying (n=2), and after 1 (n=1), 3 (n=1), 6 (n=2) or 9 (n=2) months storage at 45°C, 37°C, 20°C, 4°C or -20 °C, using the FVIII chromogenic assay, as described in the methods section. The FVIII activity of the plasma sample before lyophilisation was also measured relative to the WHO 6th IS and gave a value of 0.42 IU/ml [95%CL: 0.38 – 0.46].

Figure 4a illustrates FVIII potencies measured relative to the WHO 6th IS, for 6 months storage and, as expected, FVIII potency decreased during storage especially at the highest temperature (37°C and 45°C). Furthermore, the graph indicates a marked difference between the 2 freeze drying techniques with the VISF technique showing higher potencies compared to spontaneously frozen samples. This is reflected in greater % loss in potency (i.e. potencies relative to pre-freeze-drying liquid samples) for the spontaneously frozen samples compared to VISF samples, see Figure 4b.

Furthermore, the residual FVIII potencies for ampoules stored at +4°C, +20°C, +37°C and +45°C, for the two different freezing protocols, were expressed relative to ampoules stored at -20°C using an arbitrary value

1.00 for the -20°C ampoules. The Arrhenius model was then fitted to the data to obtain predictions of the expected loss in potency over time. Figure 5 shows the Arrhenius plot (logarithm of rate vs. inverse of temperature) for FVIII degradation observed during storage after spontaneous nucleation (blue) and vacuum induced surface freezing (red). The experimental points have been fitted with a line, and the R^2 values obtained are good, pointing towards an Arrhenius behavior. While non-Arrhenius aggregation has sometimes been observed (Wang and Roberts, 2013), the Arrhenius kinetics has often been found to be valid for lyophilized products (Wang et al., 2009; Duddu and Dal Monte, 1997; Breen et al., 2001; Perez-Moral et al. 2010). Indeed in a study on behalf of the Scientific & Standardisation Committee of the International Society on Thrombosis and Haemostasis Hubbard et al. demonstrated not only that the Arrhenius model was a good fit for lyophilised plasma with four coagulation factor markers, but also that factor VIII was the most labile of the factors studied (Hubbard et al., 2010).

The predicted mean % loss per year, based on above data after 9 months storage at the different elevated temperatures, for the VISF technique and the spontaneous nucleation, were calculated and are shown in Table 3.

Table 3. Mean predicted degradation rates expressed as % loss per year after storage for 9 months.

Chromogenic FVIII Potency Method	[§] Mean predicted % loss per year [95% upper confidence limits of predicted loss]			
	-20°C	+4°C	+20°C	+37°C
Spontaneous Nucleation	0.001 [0.001]	0.198 [0.382]	5.994 [8.598]	80.216 [80.702]
Controlled (VISF) Nucleation	0.000 [0.000]	0.003 [0.009]	0.640 [1.155]	60.951 [66.728]

[§]These results are based on stability data obtained from 4 time points over a 9-months period.

The predicted % loss in FVIII potency per year tended to be greater for the spontaneous nucleation compared to controlled nucleation (e.g. 0.198 vs 0.003 respectively for storage at +4°C). These results indicate a greater stability of the FVIII molecule in human plasma, when freeze dried under controlled (VISF) nucleation compared to spontaneous nucleation.

3.3 Reconstitution times

The reconstitution time is a crucial parameter for all pharmaceutical lyophilizates, and the freeze drying process should be designed so as to deliver a suitable reconstitution step. In this work, the reconstitution time of freeze-dried plasma was measured after storage at different temperatures for 1, 3, 6 or 9 months, in the case of both controlled and spontaneously nucleated samples. Reconstitution time of freeze-dried plasma WHO Reference Standard (07/316) was also obtained for comparison.

The results of this analysis are reported in Table 4 and indicate a remarkable improvement in reconstitution time when the VISF technique was applied. This is evident already for the case of storage at low temperature, where VISF approximately halved the reconstitution time. For instance, it took about 4, 5.2 and 7.7 min to obtain a clear solution from the VISF samples stored for 6 months at -20 °C, 4 °C or 20 °C, respectively, while the corresponding times for conventional freezing were 11.7, 15.3 and 15.4 min. Similar improvements in reconstitution times of VISF technique were observed when compared to reconstitution times of the WHO reference standard (07/316). For samples stored at higher high temperatures (37°C or 45°C), the freeze-dried bulk can harden, forming insoluble clumps and the sample can become compacted and difficult to solubilize with water. This was observed with some samples, albeit less so with the VISF technique compared to conventional freeze-drying, where reconstitution with water did not occur within 25 minutes (Table 4).

Table 4. Reconstitution times (n=1) of freeze dried cakes after storage at controlled temperature.

Time months	Reconstitution Times, min										
	-20 °C storage			4 °C storage		20 °C storage		37 °C storage		45 °C storage	
	Spon.	VISF	Ref. Std	Spon.	VISF	Spon.	VISF	Spon.	VISF	Spon.	VISF
1	13.5	7.0	12.3	-	-	-	-	21^	20	#	22
3	10.6	5.5	11.5	-	-	-	-	22	20	#	#
6	11.7	4.0	10.0	15.3	5.2	15.4	7.7	#	20.8^	-	-
9	11.5	5.0	10.4	-	-	15.0	10.5	-	-	#	20^

^ Some insoluble clumps still present

Did not reconstitute within 25 min

- Reconstitution not carried out

4. DISCUSSION

In previous studies, application of the depressurization technique to lactate dehydrogenase (Fang et al., 2018) reduced the degradation of LDH during the freezing process, but did not markedly improve protein stability during the entire freeze-drying process. Controlled nucleation by depressurization was also reported to suppress glass fogging, i.e., the undesired migration of protein solutions up on the inner walls of glass vials during the freezing step of lyophilization, and to result in higher stability against shaking stress (Singh et al., 2018). Application of the ice-fog technique (Vollrath et al., 2018) to lyophilized monoclonal antibody formulations stored at different temperatures reduced particle formation in highly concentrated systems. However, the addition of polysorbates resulted in an overall lower particle level, with no further advantage of controlled nucleation on protein stability. At low concentration, no difference with respect to particle formation between the controlled and spontaneously nucleated samples was detected. These results are in line with our previous study (Oddone et al., 2020), where HPLC-SEC and a cell-based potency assay seemed to give evidence for no dramatic difference in the behaviour of hGH at low concentration when either VISF or spontaneous nucleation were used. Our results for the highly concentrated plasma system, combined with previously published data reporting a negligible effect of controlled nucleation on protein stability in low concentrated systems (Oddone et al., 2020; Vollrath et al., 2018), seem to suggest that the benefits of controlled nucleation may depend on concentration. This result represents an interesting observation, that warrants further investigation.

However, the results obtained for FVIII activity in this work seem to indicate a difference between the two freezing protocols, with the VISF technique resulting not only in improved process efficiency, but also in enhanced protein stability. This reduced loss in protein activity may be related to the smaller ice-water interface resulting from application of controlled nucleation. As evident from the SEM images and the BET analysis, the VISF technique promoted the formation of structures having larger ice crystals, that expose a reduced surface area compared to spontaneously nucleated samples. As a result, the risk that the protein adsorbs and denatures at the ice interface is reduced, likely promoting the observed preservation of the native structure. It must also be borne in mind that FVIII is a much larger multi-domain protein with complex intermolecular interactions which can impact on its activity, and so direct comparison to a small protein like hGH (Oddone et al., 2020) may not be appropriate. An Arrhenius-based model for measuring stability was used [Kirkwood 1977,1984, Kirkwood et al 1984] for convenience and comparison between the two preparation are drawn. However, non-Arrhenius based models have been used by others [Jameel et al 2009].

When storage at high temperature is considered, application of the VISF technique made it possible to reconstitute samples that would not return to a liquid, clump-free solution if freeze dried by conventional freezing.

For instance, the VISF sample stored for 1 month at 45 °C could be reconstituted, while this was not possible in the case of conventional freezing (see Table 4). Similarly, it was possible to reconstitute the sample frozen by controlled nucleation and then stored for 6 months at 37 °C, even though some insoluble clumps were still present after 25 min, while the same result could not be achieved in the case of spontaneous freezing.

When rehydrating a freeze dried product, the gas within the pores should be displaced by the reconstitution medium so as to allow wetting of the cake. Afterwards, hydration of the solid may take place. A large pore size may promote the displacement of gas from the cake, and this is probably the reason for the observed behaviour. This same explanation was proposed in a previous work (Geidobler et al., 2013), where application of the ice-fog technique shortened the reconstitution time of highly-concentrated protein formulations. A similar reduction in reconstitution time was observed when the depressurization technique was applied to highly concentrated monoclonal antibody solutions (Singh et al., 2018).

Overall, the benefits observed when using controlled (VISF) nucleation (compared to spontaneous nucleation) in the freeze drying process of plasma (i.e. increased stability and quicker reconstitution) are likely to be extremely important in the development of reference plasma standards and reagents. Although in this work the lyophilised plasma is a reference material and the shorter reconstitution time is therefore purely a convenience, faster reconstitution of therapeutic plasma-derived products would be of enormous clinical benefit, in particular in on-demand treatment.

5. CONCLUSIONS

Two different freezing protocols, with or without the possibility to control the nucleation temperature, have been used to freeze dry human plasma. A degradation study has been subsequently performed, and both the potency of FVIII and the reconstitution time have been measured in ampoules stored at different temperatures for up to 9 months. Overall, our results suggest that the controlled nucleation approach results in reduced primary drying time, because it promotes the formation of larger pores within the dried cake. The difference in cake morphology between the two freezing protocols also accounts for the improvement in reconstitution time in samples obtained by controlled nucleation. The easier displacement of gas from larger pores allows an easier dissolution of the highly concentrated plasma lyophilizate. At the same time, the

smaller ice-water surface area when pores are large minimizes the risk of protein adsorption, and denaturation, at the ice interface. This may be at the basis of the improvement in FVIII potency for ampoules obtained by the VISF technique. Combined with previously published data, our findings suggest that the benefits of controlled nucleation on protein stability may be more pronounced for highly concentrated systems. This is an interesting finding and will be the subject of future investigations.

ACKNOWLEDGEMENTS

The Italian Ministry for Research and University is gratefully acknowledged for the PhD studentship to Andrea Arsiccio. Chiara Vitale Brovarone, Sonia Fiorilli, Carlotta Pontremoli and Claudia Udrescu are thankfully acknowledged for their help with BET analyses.

REFERENCES

Abdul-Fattah, A.M., Lechuga-Ballesteros, D., Kalonia, D.S., Pikal, M.J., 2008. The impact of drying method and formulation on the physical properties and stability of methionyl human growth hormone in the amorphous solid state. J. Pharm. Sci. 97, 163-184.

Allain JP, Friedli H, Morgenthaler JJ, Pflugshaupt R, Gunson HH, Lane RS, Myllylä G, Rock GA, Stryker MH, Woods KR, 1983. International Forum: What are the critical factors in the production and quality control of frozen plasma intended for direct transfusion or for fractionation to provide medically needed labile coagulation factors. Vox Sang. 44, 246–259

Arsiccio, A., Barresi, A.A., De Beer, T., Oddone, I., Van Bockstal, P-J., Pisano, R., 2018. Vacuum induced surface freezing as an effective method for improved inter- and intra-vial product homogeneity. Eur. J. Pharm. Biopharm. 128, 210-219.

Arsiccio, A., Sparavigna, A.C., Pisano, R., Barresi, A. A., 2019. Measuring and predicting pore size distribution of freeze-dried solutions. Dry. Technol. 37, 435-447.

Assay of human coagulation factor VIII, monograph 2.7.4. Ph. Eur. 8th edition. Strasbourg, France: Council of Europe; 2014.

Awotwe-Otoo, D., Agarabi, C., Read, E.K., Lute, S., Brorson, K.A., Khan, M.A., Shah, R.B., 2013. Impact of controlled ice nucleation on process performance and quality attributes of a lyophilized monoclonal antibody. Int. J. Pharm. 450, 70-78.

Bhatnagar, B.S., Pikal, M.J., Robin, H.B., 2008. Study of the individual contributions of ice formation and freeze-concentration on isothermal stability of lactate dehydrogenase during freezing. J. Pharm. Sci. 97, 798-814.

Breen, E.D., Curley, J.G., Overcashier, D.E., Hsu, C.C., Shire, S.J., 2001. Effect of moisture on the stability of a lyophilized humanized monoclonal antibody formulation. Pharm. Res. 18, 1345-1353.

Brower, J., Lee, R., Wexler, E., Finley, S., Caldwell, M., Studer, P., 2015. New developments in controlled nucleation: Commercializing VERISEQ® nucleation technology, in Varshney, D., Singh, M. (Eds.), Lyophilized Biologics and Vaccines. Springer, New York.

Bursac, R., Sever, R., Hunek, B., 2009. A practical method for resolving the nucleation problem in lyophilization. Bioproc. Int. 7, 6672.

436 Capozzi, L.C., Pisano, R., 2018. Looking inside the black box: Freezing engineering to ensure the quality of
437 freeze dried biopharmaceuticals. Eur. J. Pharm. Biopharm. 129, 58-65.

438 Carlebjörk G, Blombäck M, Pihlstedt P, 1986. Freezing of plasma and recovery of factor VIII. Transfusion.
439 26, 159–162.

440 Chang, B.S., Kendrick, B.S., Carpenter, J.F., 1996. Surface-induced denaturation of proteins during freezing
441 and its inhibition by surfactants. J. Pharm. Sci. 85, 1325-1330.

442 Council of Europe European Pharmacopoeia Commission: European Pharmacopoeia 8.2, 2014.
443 Monograph 2.7.4 Assay of human coagulation factor VIII. Strasbourg.

444 Duddu, S.P., Dal Monte, P.R., 1997. Effect of glass transition temperature on the stability of lyophilized
445 formulations containing a chimeric therapeutic monoclonal antibody. Pharm Res. 14, 591-595.

446 Fang, R., Tanaka, K., Mudhivarthi, V., Bogner, R.H., Pikal, M.J., 2018. Effect of controlled ice nucleation on
447 stability of lactate dehydrogenase during freeze-drying. J. Pharm. Sci. 107, 824-830.

448 Fissore, D., Pisano, R., Barresi, A., 2019. Freeze drying of pharmaceutical products. CRC Press, Boca
449 Raton, Florida, USA. pp. 1-192.

450 Franks, F., 1995. Protein destabilization at low temperatures. Adv. Protein Chem. 46, 105-139.

451 Franks, F., Auffret, T., 2009. Freeze drying of pharmaceuticals and biopharmaceuticals: Principles and
452 practice. RSC publishing, Cambridge, UK, pp. 1-206.

453 Garidel, P., Presser, I., 2019. Lyophilization of high-concentration protein formulations, in Ward, K.,
454 Matejtschuk, P. (Eds.), Lyophilization of Pharmaceuticals and Biologicals. Methods in Pharmacology
455 and Toxicology. Humana Press, New York.

456 Gasteyer, T.H., Sever, R.R., Hunek, B., Grinter, N., Verdone, M.L., May 2017. Lyophilization system and
457 method. US Patent 9651305 B2.

458 Geidobler, R., Mannschedel, S., Winter, G., 2012. A new approach to achieve controlled ice nucleation of
459 supercooled solutions during the freezing step in freeze drying. J. Pharm. Sci. 101, 4409-4413.

460 Geidobler, R., Winter, G., 2013. Controlled ice nucleation in the field of freeze drying: Fundamentals and
461 technology review. Eur. J. Pharm. Biopharm. 85, 214-222.

462 Geidobler, R., Konrad, I., Winter, G., 2013. Can controlled ice nucleation improve freeze drying of highly-
463 concentrated protein formulations? J. Pharm. Sci. 102, 3915-3919.

464 Goshima, H., Do, G., Nakagawa, K., 2016. Impact of ice morphology on design space of pharmaceutical
465 freeze-drying. J. Pharm. Sci. 105, 1920-1933.

466 Grassini, S., Pisano, R., Barresi, A.A, Angelini, E., Parvis, M., 2016. Frequency domain image analysis for
467 the characterization of porous products. Measurement 94, 515-522.
468 Hottot, A., Vessot, S., Andrieu, J., 2007. Freeze drying of pharmaceuticals in vials: Influence of freezing
469 protocol and sample configuration on ice morphology and freeze-dried cake texture. Chem. Eng.
470 Process. 46, 666-674.
471 Hubbard, A.R., Kitchen, S., Beeharry, M., Bevan, S.A., Bowyer, A., 2011. Long term stability of the Scientific
472 and Standardisation Committee Secondary Coagulation Standard (SSC Lot no 3). J. Thromb.
473 Haemost. 9, 1246-1248.
474 Human coagulation factor VIII, monograph 0275. Ph. Eur. 8th Edition. Strasbourg, France: Council of
475 Europe; 2014.
476 Jameel F, Tchessalov S, Bjornsen E, Lu X, Bersman M, Pikal MJ. Development of a freeze dried
477 biosynthetic Factor VIII: I. A case study in the optimization of formulation. Pharm Dev Technol
478 2009;14:687-97.
479 Kasper, J.C., Friess, W.F., 2011. The freezing step in lyophilization: Physico-chemical fundamentals,
480 freezing methods and consequences on process performance and quality attributes of
481 biopharmaceuticals. Eur. J. Pharm. Biopharm. 78, 248-263.

482 Kirkwood, T.B.L., 1977. Predicting the stability of biological standards and products. Biometrics 33, 736-742.
483 Kirkwood, T.B.L., 1984. Design and analysis of accelerated degradation tests for the stability of biological
484 standards III. Principles of design. J. Biol. Stand. 12, 215-224.
485 Kirkwood, T.B.L., Tydeman, M.S., 1984. Design and analysis of accelerated degradation tests for the stability
486 of biological standards II. A flexible computer program for data analysis. J. Biol. Stand. 12, 207-214.
487 Konstantinidis, A.K., Kuu, W., Otten, L., Nail, S.L, Sever, R.R., 2011. Controlled nucleation in freeze drying:
488 Effects on pore size in the dried product layer, mass transfer resistance, and primary drying rate. J.
489 Pharm. Sci. 100, 3453-3470.
490 Kramer, M., Sennhenn, B., Lee, G., 2002. Freeze drying using vacuum-induced surface freezing. J. Pharm.
491 Sci. 91, 433-443.
492 Lewis, L., Johnson, R.E., Oldroyd, M.E., Ahmed, S.S., Joseph, L., Saracovan, I., Sinha, S., 2010.
493 Characterizing the freeze drying behavior of model protein formulations. AAPS PharmSciTech 11,
494 1580-1590.

495 Ling, W. Controlled Nucleation During Freezing Step of Freeze Drying Cycle Using Pressure Differential Ice

Fog Distribution. Patent US 8839528 B2, September 23, 2014. Patent EP 2702342 B1, April 20, 2014.

Liu, J., Viverette, T., Virgin, M., Anderson, M., Paresh, D., 2005. A study of the impact of freezing on the lyophilization of a concentrated formulation with a high fill depth. Pharm. Dev. Technol. 10, 261-272.

Oddone, I., Pisano, R., Bullich, R., Stewart, P., 2014. Vacuum-induced nucleation as a method for freeze-drying cycle optimization. Ind. Eng. Chem. Res. 53, 18236-18244.

Oddone, I., Van Bockstal, P-J., De Beer, T., Pisano, R., 2016. Impact of vacuum-induced surface freezing on inter- and intra-vial heterogeneity. Eur. J. Pharm. Biopharm. 103, 167-178.

Oddone, I., Barresi, A.A., Pisano, R., 2017. Influence of controlled ice nucleation on the freeze drying of pharmaceutical products: The secondary drying step. Int. J. Pharm. 524, 134-140.

Oddone, I., Arsiccio, A., Duru, C., Malik, K., Ferguson, J., Pisano, R., Matejtschuk, P., 2020. Vacuum induced surface freezing for the freeze drying of the human growth hormone: How does nucleation control affect protein stability? J. Pharm. Sci. 109, 254-263.

Patel, S., Bhugra, C., Pikal, M., 2009. Reduced pressure ice fog technique for controlled ice nucleation during freeze drying. AAPS PharmSciTech 10, 1406−1411.

Patel, S.M., Takayuki, D., Pikal, M.J., 2010. Determination of end point of primary drying in freeze drying process control. AAPS PharmSciTech 11, 73-84.

Pérez-Moral, N., Adnet, C., Noel, T.R., Parker, R. 2010. Characterization of the rate of thermally-induced aggregation of β-lactoglobulin and its trehalose mixtures in the glass state. Biomacromolecules 11, 2985-2992.

Pikal, M.J., Rambhatla, S., Ramot, R., 2002. The impact of the freezing stage in lyophilization: Effects of the ice nucleation temperature on process design and product quality. Am. Pharm. Rev. 5, 48-53.

Pisano, R., 2019. Alternative methods of controlling nucleation in freeze drying, in Ward, K., Matejtschuk, P. (Eds.), Lyophilization of Pharmaceuticals and Biologicals. Methods in Pharmacology and Toxicology. Humana Press, New York.

Privalov, P.L., 1990. Cold denaturation of proteins. Crit. Rev. Biochem. Mol. Biol. 25, 281-305.

Rambhatla, S., Ramot, R., Bhugra, C., Pikal, M.J., 2004. Heat and mass transfer scale-up issues during freeze drying, Part 2: Control and characterization of the degree of supercooling. AAPS PharmSciTech 5, e58.

525 Rey, L., May, J.C., 2010. Freeze drying/lyophilization of pharmaceutical and biological products, 3rd edition.
526 Informa Healthcare, London, UK, pp. 1-564.
527 Searles, J., Carpenter, J., Randolph, T., 2001. The ice nucleation temperature determines the primary drying
528 rate of lyophilization for samples frozen on a temperature-controlled shelf. J. Pharm. Sci. 90, 860-871.
529 Shire, S.J., Shahrokh, Z., Liu, J., 2004. Challenges in the development of high protein concentration
530 formulations. J. Pharm. Sci. 93, 1390-1402.
531 Singh, S.N., Kumar, S., Bondar, V., Wang, N., Forcino, R., Colandene, J., Nesta, D., 2018. Unexplored
532 benefits of controlled ice nucleation: Lyophilization of a highly concentrated monoclonal antibody
533 solution. Int. J. Pharm. 552, 171-179.
534 Strambini, G.B., Gabellieri, E., 1996. Proteins in frozen solutions: Evidence of ice-induced partial unfolding.
535 Biophys. J. 70, 971-976.
536 Swärd-Nilsson, A.M., Persson, P.O., Johnson, U., Lethagen, S., 2006. Factors influencing factor VIII activity
537 in frozen plasma. Vox Sang. 90, 33–39.
538 Takahashi H, Hanano M, Tatewaki W, Shibata A., 1986. Factor VIII lability, protein C and other vitamin K-
539 dependent proteins. Thromb Res. 43(5), 561-8.
540 Umbach, M. Freeze Drying Plant. Patent EP 3093597 B1, December 27, 2017.
541 Vollrath, I., Friess, W., Freitag, A., Hawe, A., Winter, G., 2018. Does controlled nucleation impact the
542 properties and stability of lyophilized monoclonal antibody formulations? Eur. J. Pharm. Biopharm.
543 129, 134-144.
544 Vollrath, I., Friess, W., Freitag, A., Hawe, A., Winter, G., 2019. Comparison of ice fog methods and
545 monitoring of controlled nucleation success after freeze-drying. Int. J. Pharm. 558, 18-28.
546 Wang, W., Roberts, C.J., 2013. Non-Arrhenius protein aggregation. AAPS J. 15, 840-851.
547 Wang, B., Tchessalov, S., Cicerone, M.T., Warne, N.W., Pikal, M.J. 2009. Impact of sucrose level on storage
548 stability of proteins in freeze-dried solids: II. Correlation of aggregation rate with protein structure and
549 molecular mobility. J Pharm Sci. 98, 3145-3166.
550 Ward, K., Matejtschuk, P., 2019. Lyophilization of pharmaceuticals and biological: New technologies and
551 approaches. Methods in Pharmacology and Toxicology. Humana Press, New York, pp. 1-382.
552

553 **LIST OF FIGURES**

554

555 Figure 1: Representative profiles of fluid temperature and chamber pressure during application of the VISF
556 protocol. The sample is first equilibrated at T_n, and nucleation is then induced by lowering the pressure to a
557 formulation-specific value. A second holding stage at T_m is subsequently performed to promote the growth of
558 large ice crystals.

559

560 Figure 2: Temperature and pressure profiles during a) the spontaneous run and b) the VISF run for the
561 plasma batch. Black line: fluid temperature, Red line: Product temperature, Green line: capacitance
562 manometer, Blue line: Pirani manometer. In panel a, an enlargement of the product temperature during
563 freezing is shown in the inset.

564

565 Figure 3: SEM images of the samples obtained after spontaneous (top) and controlled (bottom) nucleation.
566 The magnification is the same for all images, and the white bar in the figure corresponds to a distance of 100
567 µm.

568

569 Figure 4: (a) FVIII potency (IU/ml) measured relative to the WHO 6th IS FVIII/VWF Plasma (07/316) after 6
570 months storage at different accelerated degradation temperatures, for samples freeze dried with
571 spontaneous (open circles) or controlled VISF (filled circles) nucleation. (b) Percentage (%) loss in FVIII
572 potency post freeze-dried samples (i.e. relative to pre-freeze-drying liquid samples) with spontaneous (open
573 circles) or controlled (filled circles) nucleation, after 6 months storage at different accelerated degradation
574 temperatures. The error bars displayed in the figure correspond to standard deviation.

575

576 Figure 5: Arrhenius plot (logarithm of rate lnk vs. inverse of temperature 1/T) for FVIII degradation observed
577 during storage after spontaneous nucleation (blue) and vacuum induced surface freezing (red). The
578 experimental points, represented as blue squares or red triangles, have been fitted with a line. The equation
579 and R^2 value of the fitting are also displayed on the graph.

580
581
582

583

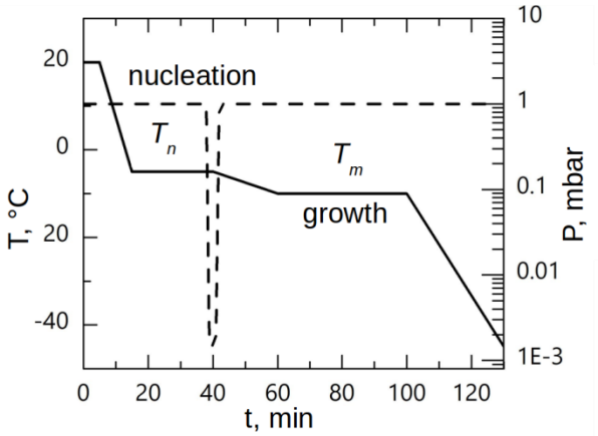

584
585
586 Figure 1

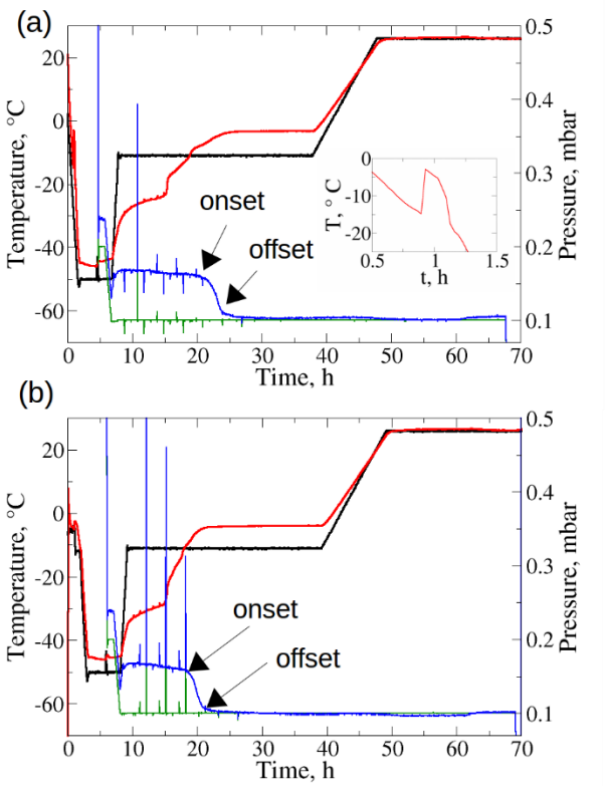
(a)
Temperature, °C
Pressure, mbar
Time, h
onset
offset
T, ° C
t, h
(b)
Temperature, °C
Pressure, mbar
Time, h
onset
offset

Figure 2

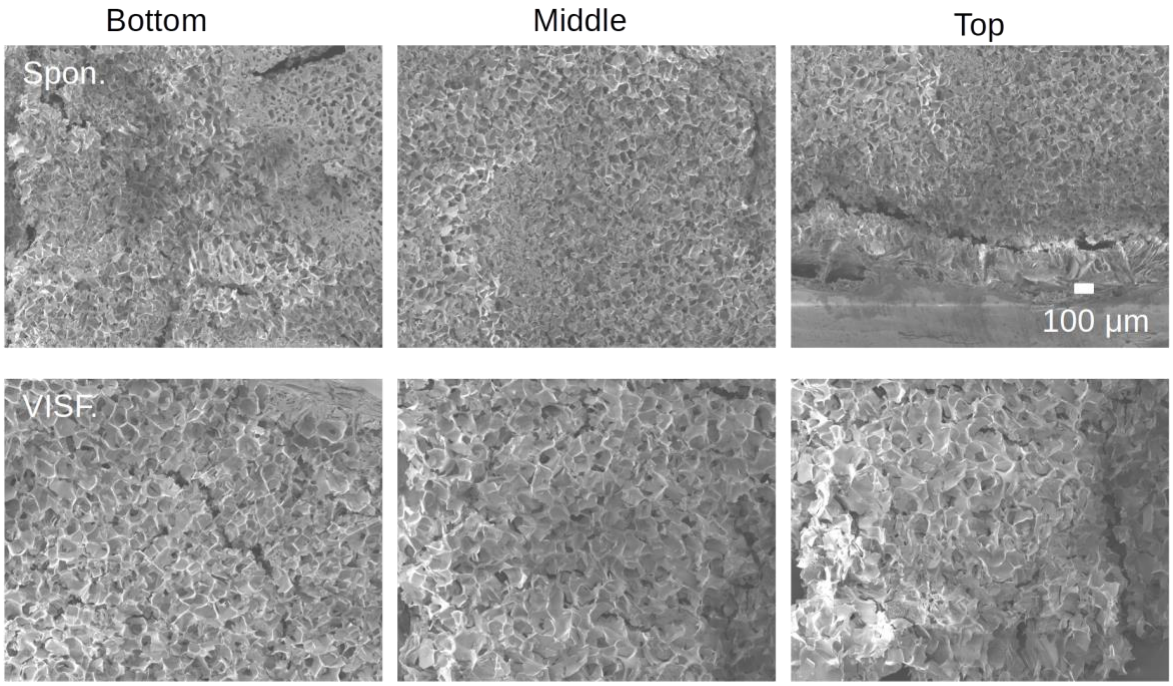

Figure 3

(a)

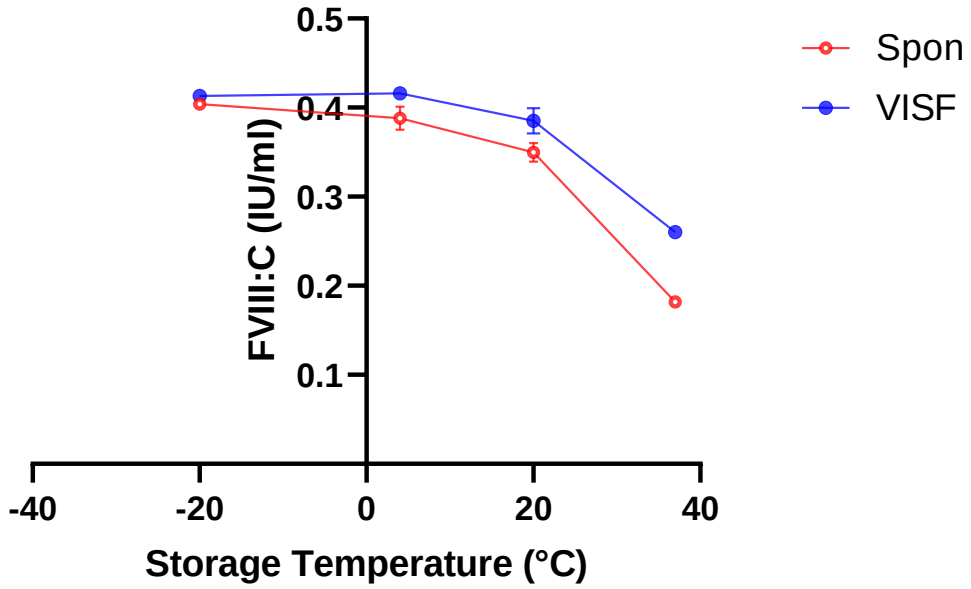

621

622
623
624

625

(b)

628

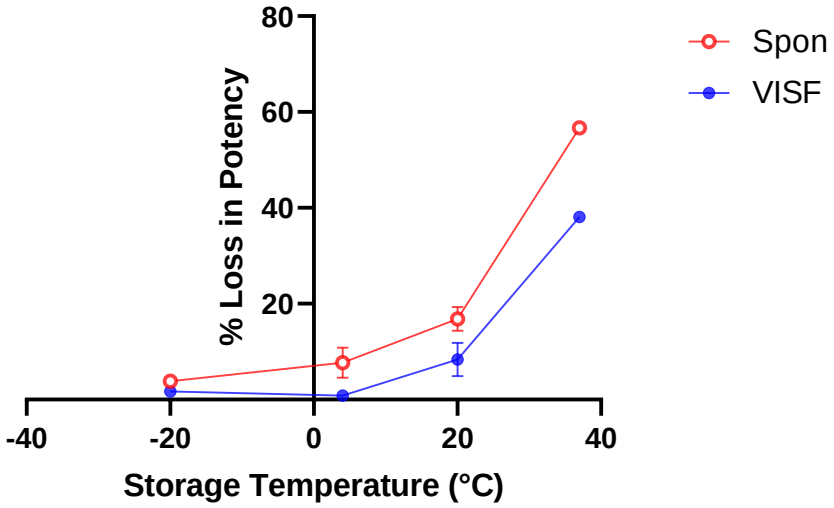

629
630
631
632
633
634

Figure 4

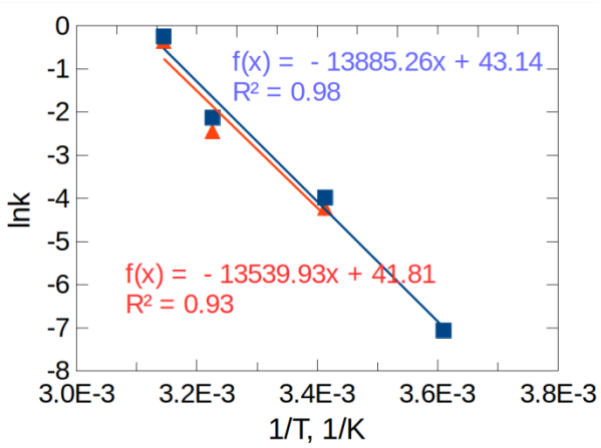
f(x) = - 13885.26x + 43.14
R² = 0.98
f(x) = - 13539.93x + 41.81
R² = 0.93
lnk
1/T, 1/K
0
-1
-2
-3
-4
-5
-6
-7
-8
3.0E-3
3.2E-3
3.4E-3
3.6E-3
3.8E-3

Figure 5